

Provided for non-commercial research and education use.
Not for reproduction, distribution or commercial use.

	Volume 36	Issue 3	March 2009	ISSN 0734-743X
International Journal of IMPACT ENGINEERING				
Editor-in-Chief Magnus LANGSETH				
Contents				
D. Varas, R. Zaera and J. López-Puente	363	Numerical modelling of the hydrodynamic ram phenomenon		
H. Chai and G. Ravichandran	375	On the mechanics of fracture in monoliths and multilayers from low-velocity impact by sharp or blunt-tip projectiles		
M. Grujic, B. Pandurangan, N. Coutris, B.A. Cheeseman, C. Fountzoulas, P. Patel, D.W. Templeton and K.D. Bishnoi	386	A simple ballistic material model for soda-lime glass		
X.W. Zhang, H. Su and T.X. Yu	402	Energy absorption of an axially crushed square tube with a buckling initiator		
E.W. Andrews and N.A. Moussa	418	Failure mode maps for composite sandwich panels subjected to air blast loading		
T. Børvik, M.J. Forrestal, O.S. Hopperstad, T.L. Warren and M. Langseth	426	Perforation of AA5083-H116 aluminium plates with conical-nose steel projectiles – Calculations		
Y. Liu, A. Ma and F. Huang	438	Numerical simulations of oblique-angle penetration by deformable projectiles into concrete targets		
<i>Contents continued on OBC....</i>				
Available online at  www.sciencedirect.com				

This article appeared in a journal published by Elsevier. The attached copy is furnished to the author for internal non-commercial research and education use, including for instruction at the authors institution and sharing with colleagues.

Other uses, including reproduction and distribution, or selling or licensing copies, or posting to personal, institutional or third party websites are prohibited.

In most cases authors are permitted to post their version of the article (e.g. in Word or Tex form) to their personal website or institutional repository. Authors requiring further information regarding Elsevier's archiving and manuscript policies are encouraged to visit:

<http://www.elsevier.com/copyright>



Contents lists available at ScienceDirect

International Journal of Impact Engineering

journal homepage: www.elsevier.com/locate/ijimpeng

Impact performance of W-beam guardrail installed at various flare rates

John D. Reid*, Beau D. Kuipers, Dean L. Sicking, Ronald K. Faller

Midwest Roadside Safety Facility, N104 WSEC (0656), University of Nebraska, Lincoln, NE 68588, USA

ARTICLE INFO

Article history:

Received 13 June 2007

Received in revised form 12 August 2008

Accepted 17 August 2008

Available online 19 September 2008

Keywords:

Roadside safety
W-beam guardrail
Crash analysis
Flare rates

ABSTRACT

The potential to increase suggested flare rates for strong post, W-beam guardrail systems and thus reduce guardrail installation lengths is investigated. This reduction in length would result in decreased guardrail construction and maintenance costs, and reduce impact frequency. If the W-beam guardrail can withstand the higher impact angles, with only modest increases in accident severity, total accident costs can be reduced. Computer simulation and five full-scale crash tests were completed to evaluate increased flare rates up to, and including, 5:1. Computer simulations indicated that conventional G4(1S) guardrail modified to incorporate a routed wood block could not successfully meet NCHRP Report 350 crash test criteria when installed at any steeper flare rates than the 15:1 recommended in the Roadside Design Guide. However, computer modeling and full-scale crash testing showed that the Midwest Guardrail System (MGS) could meet NCHRP Report 350 impact criteria when installed at a 5:1 flare rate. Impact severities during testing were found to be greater than intended, yet the MGS passed all NCHRP 350 requirements. Hence, flaring the MGS guardrail as much as 5:1 will still provide acceptable safety performance for the full range of passenger vehicles. Increasing guardrail flare rates will reduce the overall number of guardrail crashes without significantly increasing risks of injury or fatality during the remaining crashes. Therefore, it is recommended that, whenever roadside topography permits, flare rates should be increased to as high as 5:1 when using the MGS.

© 2008 Elsevier Ltd. All rights reserved.

1. Introduction

NCHRP Report 350 defines crash testing standards that roadside hardware must satisfy in order to be approved for installation on the National Highway System [1]. In the case of strong post, W-beam guardrail systems this does not mean, however, that the installation of the guardrail must be identical to the crash testing conditions. For example, such guardrail systems are allowed to be installed with a flare up to a rate of 15:1 for high-speed applications; as opposed to the tangent installations used during crash test evaluation. This flare rate is justified because of an overall reduction in crash frequency due to the flare [2]. Reducing the number of crashes can offset modest increases in crash severity, such that total accident costs, measured in terms of injuries and fatalities, go down.

Utilizing a flared guardrail configuration effectively raises the impact severity of all roadside collisions by increasing the relative impact angle between the encroaching vehicle and the guardrail installation. The maximum flare rates currently recommended in the Roadside Design Guide are based on the performance of conventional strong post W-beam guardrail [3]. This barrier has

long been recognized as having very little reserve capacity to contain and redirect heavy passenger vehicles when impact severities increase [4,5]. The Midwest Guardrail System (MGS) has been shown to have significantly greater capacity than conventional strong post-guardrail and should provide improved performance when installed in a flared configuration.

Therefore, Midwest States Pooled Fund Program and the National Cooperative Highway Research Program (Project 17-20(3)) sponsored the research described herein to develop updated flare rate guidelines. The goal of this research was to identify the maximum flare rate at which the MGS could provide acceptable safety performance.

2. Flare rates

A thorough discussion on the history of flare rates used in roadside safety is provided by Kuipers et al. [6]. Below is a brief discussion of the relevant information for this paper.

The 2002 American Association of State Highway and Transportation Officials' (AASHTO) Roadside Design Guide (RDG) recommend maximum flare rates as a function of highway design speed and barrier type [3]. Currently, the maximum flare rate suggested for a semi-rigid barrier system is 15:1 for a 110 km/h highway design speed and slightly sharper flare rates for lower design speeds, as listed in Table 1.

* Corresponding author. Tel.: +1 402 472 3084.

E-mail address: jreid@unl.edu (J.D. Reid).

Table 1
AASHTO RDG suggested flare rates

Design speed		Barrier flare rate
(km/h)	(mph)	
110	70	15:1
100	60	14:1
90	55	12:1
80	50	11:1
70	45	10:1
60	40	8:1
50	30	7:1

Increasing maximum allowable flare rates would significantly reduce guardrail lengths whenever roadside or median slopes are relatively flat. This reduction in guardrail lengths would also reduce construction costs and reduce impact frequency [2]. Hence, a revised flare rate design has the potential to decrease construction, maintenance, and overall accident costs. An example of the reduction in guardrail length is illustrated in Fig. 1. Guardrail design placement dimensions were obtained using the following equations provided in the RDG:

$$X = \frac{L_A + (b/a)(L_1) - L_2}{(b/a) + (L_A/L_R)} \quad (1)$$

$$Y = L_A - \frac{L_A}{L_R}(X) \quad (2)$$

where X is the minimum required length of need; Y is the lateral offset; (a:b) is the desired flare rate; L_A is lateral extent of the area of concern; L_R is the runout length; L₁ is the tangent length of barrier upstream from the area of concern; L₂ is the lateral distance from the edge of the traveled way

The calculated guardrail length is then obtained directly from the X and Y values. Furthermore, it is only possible to construct guardrails in 3.8 m increments, resulting in an actual installation length that is somewhat longer than the calculated values. Applying similar techniques, results were determined for the flared section of guardrail installations for other flare rates, as listed in Table 2.

Examination of the guardrail installation lengths provided in Table 2 indicates an obvious advantage to flaring the guardrail away from the road as compared to the baseline tangent installation. A 15:1 flare reduces the installation length by one-half as compared

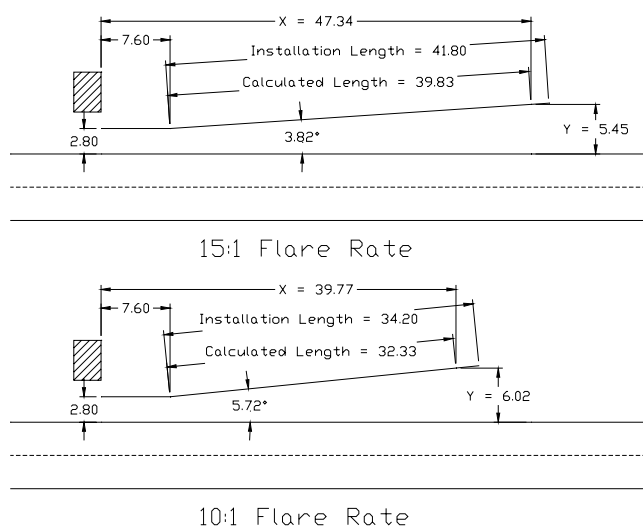


Fig. 1. Comparison of flared guardrail lengths (distances in meters).

Table 2
Guardrail installation lengths

Guardrail configuration	Flare angle (deg)	X (m)	Y (m)	Calculated guardrail length (m)	Guardrail installation length (m)
Baseline	0.00	82.67	0	82.67	83.6
15:1	3.81	47.34	5.45	39.83	41.8
14:1	4.09	46.05	5.55	38.55	41.8
13:1	4.40	44.66	5.65	37.17	38.0
12:1	4.76	43.16	5.76	35.68	38.0
11:1	5.19	41.53	5.88	34.07	34.2
10:1	5.71	39.77	6.02	32.33	34.2
9:1	6.34	37.85	6.16	30.44	34.2
8:1	7.13	35.75	6.32	28.37	30.4
7:1	8.13	33.44	6.49	26.11	26.6
6:1	9.46	30.90	6.68	23.62	26.6
5:1	11.31	28.07	6.89	20.89	22.8

to the baseline system. Furthermore, increasing the current maximum flare rate would reduce the guardrail installation length even more.

The construction length information is also important when considering an increase in the maximum flare rate. It may be possible to increase the flare rate to 10:1; however, for this example, no benefit would be gained over specifying the 11:1 flare rate.

The drawback to increasing the flare rate is that impact severities (ISs) are directly related to impact angles, as listed in Table 3. There is a significant increase in the IS going from the tangent to the roadway system (baseline case) to the currently allowable 15:1 flared rate. However, the IS does not increase rapidly with further moderate increases in the flare rate. Thus, an increase in RDG's suggested flare rate should not greatly increase the severity of guardrail impacts.

As shown above, increasing guardrail flare rates reduce the overall length of a guardrail installation. This reduction in guardrail length should produce a proportionate reduction in guardrail impacts. Hence, the overall level of safety provided should be enhanced by sharper flare rates, provided the barrier capacity is not compromised.

3. Midwest guardrail system

Two different strong post, W-beam guardrail systems were initially investigated: (1) the modified G4(1S) system, and (2) the

Table 3
Impact severities (ISs)

Guardrail orientation	Flare angle (deg)	Tests 3–10			Tests 3–11		
		Impact angle (deg)	Impact severity (kJ)	% Increase in IS	Impact angle (deg)	Impact severity (kJ)	% Increase in IS
Baseline	0.0	20	40.4	–	25	137.8	–
15:1 ^a	3.8	23.8	56.3	39	28.8	179.2	30
14:1	4.1	24.1	57.5	42	29.1	182.3	32
13:1	4.4	24.4	58.9	46	29.4	185.9	35
12:1	4.8	24.8	60.6	50	29.8	190.2	38
11:1	5.2	25.2	62.6	55	30.2	195.2	42
10:1	5.7	25.7	65.0	61	30.7	201.2	46
9:1	6.3	26.3	68.0	68	31.3	208.7	52
8:1	7.1	27.1	71.8	78	32.1	218.2	58
7:1	8.1	28.1	76.8	90	33.1	230.5	67
6:1	9.5	29.5	83.5	107	34.5	247.1	79
5:1	11.3	31.3	93.2	131	36.3	270.6	96

$$\text{Impact severity} = IS = \frac{1}{2}(\text{mass})(\text{speed} \times \sin(\text{impact angle}))^2$$

^a RDG suggested maximum flare rate for semi-rigid barrier systems on 110 km/h roadways.

^b Mass of Test 3–10 is the total of the vehicle (820 kg) and the required dummy (75 kg).



Fig. 2. MGS installed with a 7:1 flare.

Midwest Guardrail System (MGS). The MGS differs from conventional strong post-guardrails in three significant ways: (1) W-beam splices were relocated from the post to midspan between posts; (2) the top of the guardrail was raised from 706 mm to 787 mm, and (3) the depth of the blockouts on the posts was increased from 203 mm to 305 mm. This barrier has been shown to have significantly greater capacity than the standard W-beam guardrail. Details of the MGS and its compliance crash testing are reported in Refs. [5,7].

After initial analysis [6], and discussions with the Midwest Pooled Fund States, the MGS was selected for further investigation and full-scale crash testing for the flare rate study.

3.1. Test system

The MGS used for full-scale crash testing during this project consisted of: (1) simulated tangent energy absorbing terminals on both ends of the system, each with two wood posts inserted into 1.8 m long foundation tubes, (2) twenty-five W152 mm × 13.4 mm × 1829 mm long steel posts spaced 1905 mm apart, (3) 2.67 mm thick standard galvanized W-beam guardrail mounted with a top height of 787 mm, (4) 152 mm × 305 mm × 362 long wood blockouts bolted between the W-beam rail and steel posts, and (5) soil type grade B – AASHTO M 147-65. As an example, the installation constructed with a 7:1 flare rate is shown in Fig. 2.

4. Analysis

BARRIER VII [8] simulations were performed during the study for three purposes: (1) to develop an understanding of the potential behavior of a flared MGS, (2) to recommend an initial flare rate to full-scale crash test, and (3) to determine the critical impact point (CIP) prior to each full-scale crash test. The CIP is considered the worst case location for a vehicle to impact a safety device. Details of the analysis are documented by Kuipers et al. [6].

Determining critical flare rates and corresponding CIP's for each flare rate of interest turned out to be very difficult because there are no set criteria for BARRIER VII that clearly defines failure of a system. Measures traditionally used to predict propensity for guardrail failure include maximum deflection, maximum rail tension, degree of pocketing and wheel snag. It is important to note that for a given system configuration, the worst case measurements rarely line-up; for example, the impact point that results in maximum deflection would probably not be the same impact point that results in the greatest degree of pocketing. Thus, determining the critical flare rate and the corresponding CIP requires some degree of insight and engineering judgment.

Because the MGS has proven to be a very robust system for several different configurations, yet with different results than the modified G4(1S) system [6,7], the subjective criteria developed over many years of using BARRIER VII for defining critical conditions for W-beam guardrail were generally not applicable. Nonetheless, using the previous criteria and engineering judgment, design and testing decisions were made to the best of the team's ability.

LS-DYNA, a 3-D non-linear finite element code [9], was used in parallel with BARRIER VII in order to develop further insight into the behavior of a flared MGS. After the initial crash test was a success, LS-DYNA was then used before each next test to simulate the proposed higher flare rate conditions. Ultimately, the MGS model proved to be stiffer than the actual system and thus, under-predicted dynamic deflections. Nonetheless, LS-DYNA simulations provided the researchers with reasonable levels of confidence at each step in the testing process.

The LS-DYNA model of the MGS was fairly detailed but did have a few significant simplifications in order to have reasonable CPU requirements and because the technology for more accurate details has yet to be developed. The two most significant simplifications were: (1) rail rupture was modeled with a relatively coarse mesh and a failure strain in the material model; true rail rupture needs to be modeled with a very fine mesh and a fracture mechanics approach, and (2) soil simplifications were required since existing material modeling techniques for soil do not predict soil fracture shear bands allowing the soil to soften after a certain deflection,

MGS FR-4: 100.0 km/h @ 36.31 deg

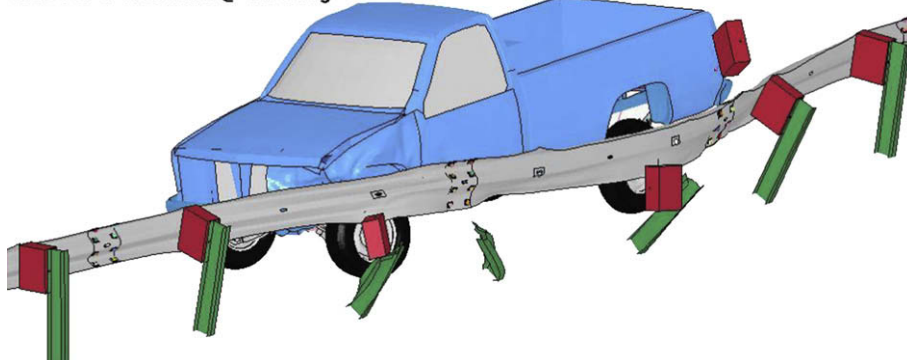


Fig. 3. Simulation results.

Table 4
Crash test results

Test	Installation flare rate		Impact angle relative to roadway [deg]		Impact angle relative to guardrail [deg]		Impact speed [km/h]		Total vehicle mass [kg]		Impact severity [kJ]		Effective flare rate	
	(a:b)	[deg]	Target	Actual	Target	Actual	Target	Actual	Target	Actual	Target	Actual	[deg]	(a:b)
FR-1	13:1	4.4	25.0	26.2	29.4	30.5	100.0	102.9	2000	2063	186	214	6.76	8.4:1
FR-2	7:1	8.1	25.0	25.9	33.1	34.0	100.0	101.6	2000	2023	230	252	9.86	5.8:1
FR-3	7:1	8.1	20.0	20.6	28.1	28.7	100.0	102.2	895	894	77	83	9.37	6.1:1
FR-4	5:1	11.3	25.0	25.5	36.3	36.8	100.0	104.7	2000	2014	270	306	14.00	4.0:1
FR-5	5:1	11.3	20.0	20.5	31.3	31.8	100.0	95.5	895	908	93	89	10.47	5.4:1

Note: all test passed NCHRP 350 requirements.

and thus allowing the post to flip out of the soil sending a wedge of soil dispersing all around the local area.

Simulation results of the pickup truck impacting a 5:1 flare rate system are shown in Fig. 3. The event time shown is just prior to the truck becoming parallel to the rail. Although wheel snag between the tire and posts was observed during the simulation, the results indicated that the snag would not cause any significant disruption to the vehicle stability or rail integrity. Additionally, no significant pocketing was evident from the simulation. Later, when this test was actually performed, test FR-4 showed very similar behavior to that predicted by the LS-DYNA model.

5. Crash testing

5.1. Test FR-1

The first full-scale crash test on a flared system, test FR-1, was performed on an MGS installed with a 13:1 flare using the 2000p vehicle. Test conditions were those of NCHRP Test 3–11 consisting of a 2000p pickup truck impacting the system at 100 km/h and at 25° relative to the roadway. The critical impact point (CIP) was determined from BARRIER VII to be 4.97 m upstream from the centerline of the splice between posts 14 and 15.

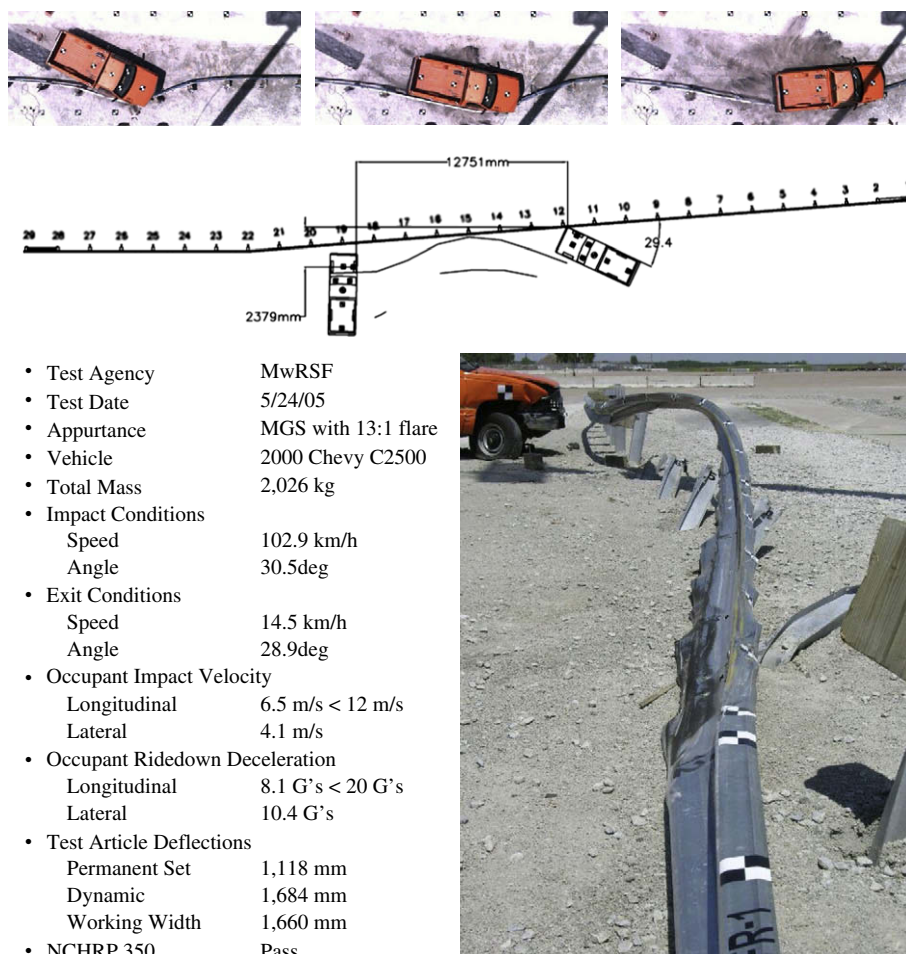


Fig. 4. Test FR-1 summary.

Results were very encouraging with the vehicle remaining stable throughout the impact event (see Table 4 and Fig. 4). Test FR-1 clearly passed all NCHRP 350 requirements. Dynamic deflection was recorded at a maximum of 1684 mm, which, under some circumstances, may seem a little high, but if there is enough space to install a flared system on relatively flat ground, then dynamic deflections are generally not a major concern.

Due to testing deviations, the actual impact of FR-1 had a higher impact angle and speed than those specified in NCHRP 350 (see Table 4). As a result, the IS was 15% higher than targeted. An effective flare rate can be calculated using the actual FR-1 impact severity, the target mass, the target speed, and the equation for the IS, as listed in Table 3. This results in an effective flare rate of 8.4:1 for FR-1.

The concept behind the effective flare rate can be stated as follows: if the test was run at the target mass and velocity, then what angle would be required in order to match the actual IS? That angle is the total effective impact angle, thus subtracting from it the target angle relative to the roadway results in the effective flare rate angle. Which can then be easily converted to the a:1 effective flare rate format.

5.2. Test FR-2

Because of the 8.4:1 effective flare rate used on FR-1, the next test, FR-2, was performed on an MGS installed with a 7:1 flare using the 2000p vehicle. The CIP was determined to be 5.24 m upstream of the splice between posts 14 and 15. Again, results were very

encouraging with the vehicle remaining stable throughout the impact (see Table 4 and Fig. 5). Test FR-2 clearly passed all NCHRP 350 requirements. For a second time, the actual impact had a higher impact angle and speed than those specified in NCHRP 350 (see Table 4). As a result, the IS was 9% higher than targeted; which can be used to calculate an effective flare rate of 5.8:1 for FR-2.

5.3. Test FR-3

Another concern for guardrail systems is NCHRP Test 3–10 consisting of an 820c small car impacting the system at 100 km/h and at 20° relative to the roadway. The CIP was determined to be 1.8 m upstream of the splice between posts 12 and 13. Although not as severe of a test as the 2000p in terms of impact severity, this test checks for things like vehicle under riding the system, wheel snag that might cause vehicle rollover, and abrupt decelerations due to pocketing in the rail.

Thus, test FR-3 was performed using an 820c vehicle on an MGS installed with a 7:1 flare rate. Results are presented in Table 4 and Fig. 6. The vehicle was smoothly redirected, remained completely stable throughout the test and showed no areas of concern. FR-3 easily passed all NCHRP 350 requirements.

5.4. Test FR-4

Next, researchers wanted to further test the limits of the MGS. After discussions with the Midwest Pooled Fund States it was decided to test the 2000p vehicle on an MGS installed with a 5:1

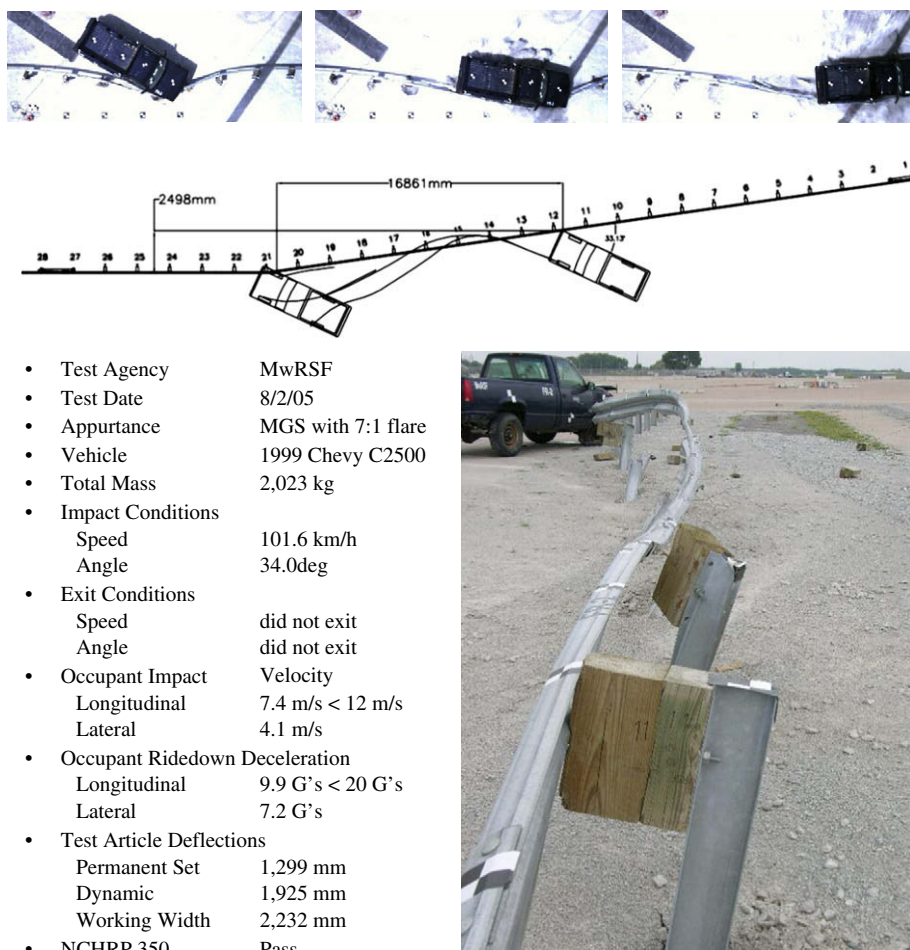


Fig. 5. Test FR-2 summary.

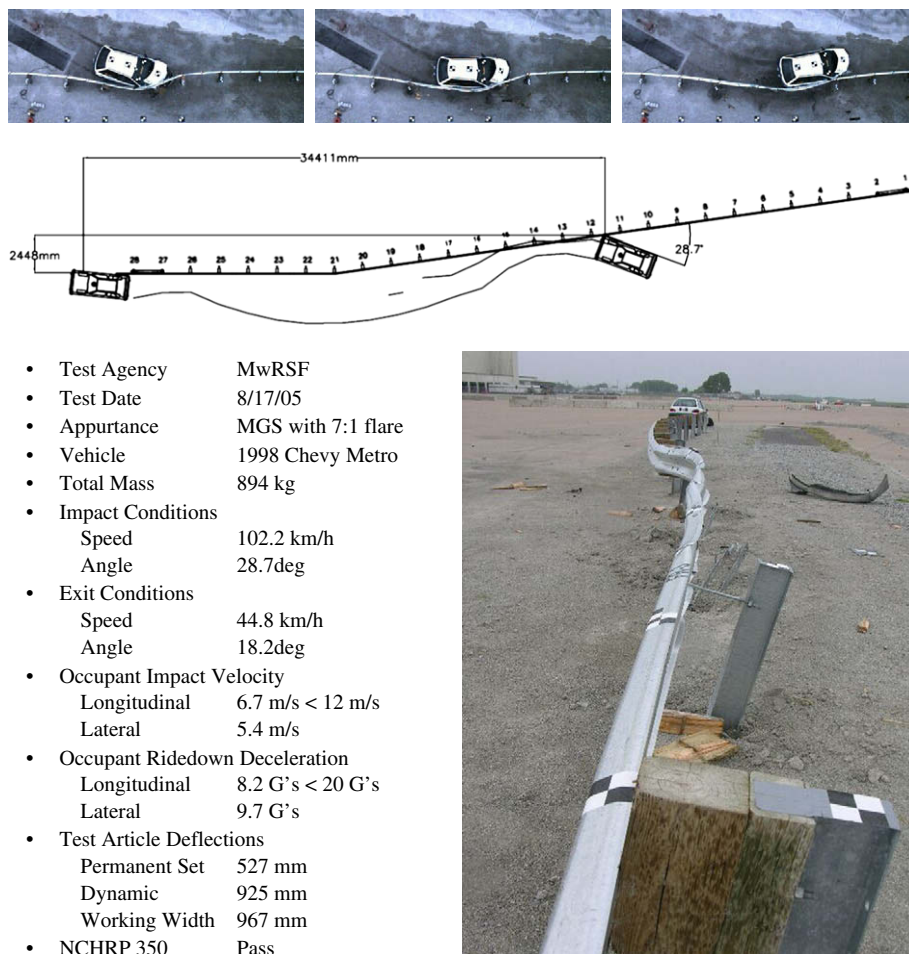


Fig. 6. Test FR-3 summary.

flare rate. The impact angle targeted for test FR-4 was 36.3° . The CIP was determined to be 5.0 m upstream of the splice between posts 14 and 15.

As might be expected the system underwent considerable damage, although not excessive, and the truck remained remarkably stable throughout the impact. Results are presented in Table 4 and Fig. 7. Dynamic deflection was measured as 1918 mm, which seemed reasonable for such a high angle of impact. Test FR-4 clearly passed all NCHRP 350 requirements.

Once again, the actual impact exceeded those specified in NCHRP 350 (see Table 4): FR-4 had a slighter higher impact angle and much higher impact speed than required. As a result, the IS was 13% higher than targeted; which can be used to calculate an effective flare rate of 4.0:1 for FR-4.

5.5. Test FR-5

To complete the testing, test FR-5 was performed using an 820c vehicle on an MGS installed with a 5:1 flare rate. The CIP was determined to be 1.43 m upstream of the splice between posts 12 and 13. Results are presented in Table 4 and Fig. 8. The vehicle's front tire snagged on three posts during the event, and on the third post, the Metro spun clockwise approximately 144° and came to rest near the system. The vehicle maintained stability throughout the event and the rail showed no signs of tearing. FR-5 passed all NCHRP 350 requirements.

In the past, some concern had been expressed about wheel snag occurring during small car testing. For the MGS, wheel snag did

indeed occur during high flare rate testing. However, this did not cause any problems during FR-5. Similarly, on the many small car tests that have been performed on the MGS, not once has wheel snag caused any problems. Thus, this issue is considered not important to the MGS.

6. Further analysis

LS-DYNA was then used to simulate even higher flare rates than those crash tested. At a flare rate of 3:1 (i.e., a 43° impact angle from the tangent), as well as 4:1, results showed that the truck to be captured and redirected. At a flare rate of 2:1 the model went numerically unstable relatively early in the event due to the large forces between the truck and the rail as a result of the severe 52° impact. Even though this additional modeling appears to indicate some additional capacity in the MGS barrier, further testing is not recommended. Increasing the flare rate beyond 5:1 would not greatly reduce overall guardrail lengths. Further, LS-DYNA cannot adequately predict rail rupture or severe damage to the suspension system on the truck. Nonetheless, these higher flare rate simulations indicate that, even when installed at a flare rate of 5:1, the MGS barrier may have some reserve capacity to accommodate vehicles impacting at higher speeds, angles, or with greater mass.

6.1. Modified G4(1S) guardrail system

The modified G4(1S) guardrail system is often considered the current standard guardrail system in the United States; hereinafter

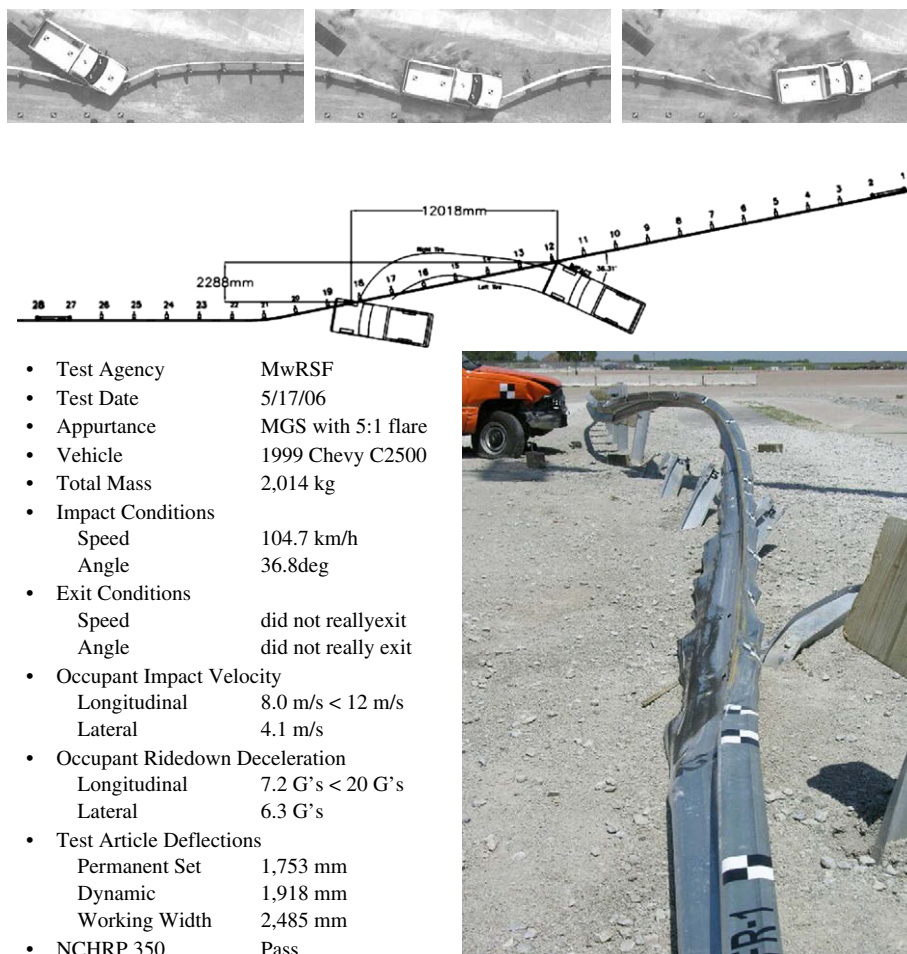


Fig. 7. Test FR-4 summary.

referred to as the G4(1S)M. The G4(1S)M is a steel post, routed wood blockout, W-beam guardrail system. As mentioned previously, the MGS, which has been the focus of this paper, is a relatively new development based on the G4(1S)M. Although full-scale crash testing of the G4(1S)M at various flare rates is not practical within the scope of this work due to costs, a limited simulation study was performed.

In 1995, TTI successfully conducted test 405421-1 according to NCHRP Report 350 Test 3-11 specifications on the G4(1S)M guardrail system [10]. The vehicle was safely redirected in a very stable manner with very little roll or pitch. Additionally, all safety criteria were well below the limits specified in Report 350.

Using information from the crash test and the LS-DYNA model of the MGS, a G4(1S)M finite element model was created. The baseline simulation, which matches TTI test 405421-1, is a pickup truck impacting the guardrail at 100 km/h and 25°. In this situation the guardrail is tangent to the roadway, which means there is no flare rate. The simulation predicted that the truck will not override the system and will be redirected in a manner similar to the actual full-scale test (see Fig. 9).

The G4(1S)M model was then used to investigate flare rates of 15-to-1, 13-to-1 and 7-to-1. The results of these simulations are shown in Fig. 9. Unlike the MGS, LS-DYNA did not predict successful performance for the G4(1S)M for steep flare conditions. Both the 13-to-1 and 7-to-1 flare rate simulations predicted that the truck would override the guardrail, which is considered a failure. Further, for the very shallow 15-to-1 flare rate, LS-DYNA predicted significant vehicle climb, even though the truck was predicted to be

successfully contained. Note that the current Roadside Design Guide allows the modified G4(1S)M system to be installed up to a 15-to-1 flare rate. These findings are consistent with other full-scale crash tests that indicate slight modifications in the G4(1S)M, such as reducing its height by 5/8 of an inch [11] or replacing the routed block with a standard block [12], often leads to vehicle climb and/or rollover. Never-the-less, full-scale crash testing would be required to verify the LS-DYNA predictions that the G4(1S)M performs poorly, even for flare rates as low as 13:1 and 15:1.

7. Practical implications

Some concern has been expressed that there may be a potential weak point in a flared guardrail associated with the beginning of the flare. The theory is that there is some delay in development of tension as the hinge point is pushed backward and that this delay may cause the guardrail to disengage from the impacting vehicle. This behavior arises whenever there is a portion of the impact during which the lateral stiffness of the barrier is essentially zero. Although this type of delayed tension has been shown to be a problem for weak post-guardrails, including cables and weak post W-beam guardrails, the high post stiffness of a strong post-guardrail assures that there is significant lateral stiffness of the barrier throughout the impact. In fact, the effective impact severity of a crash is significantly reduced when a vehicle encounters the end of the flared section. For such an impact, the vehicle does not need to be redirected to be parallel to the flared section, but instead needs only to become parallel to the tangent portion of the barrier.

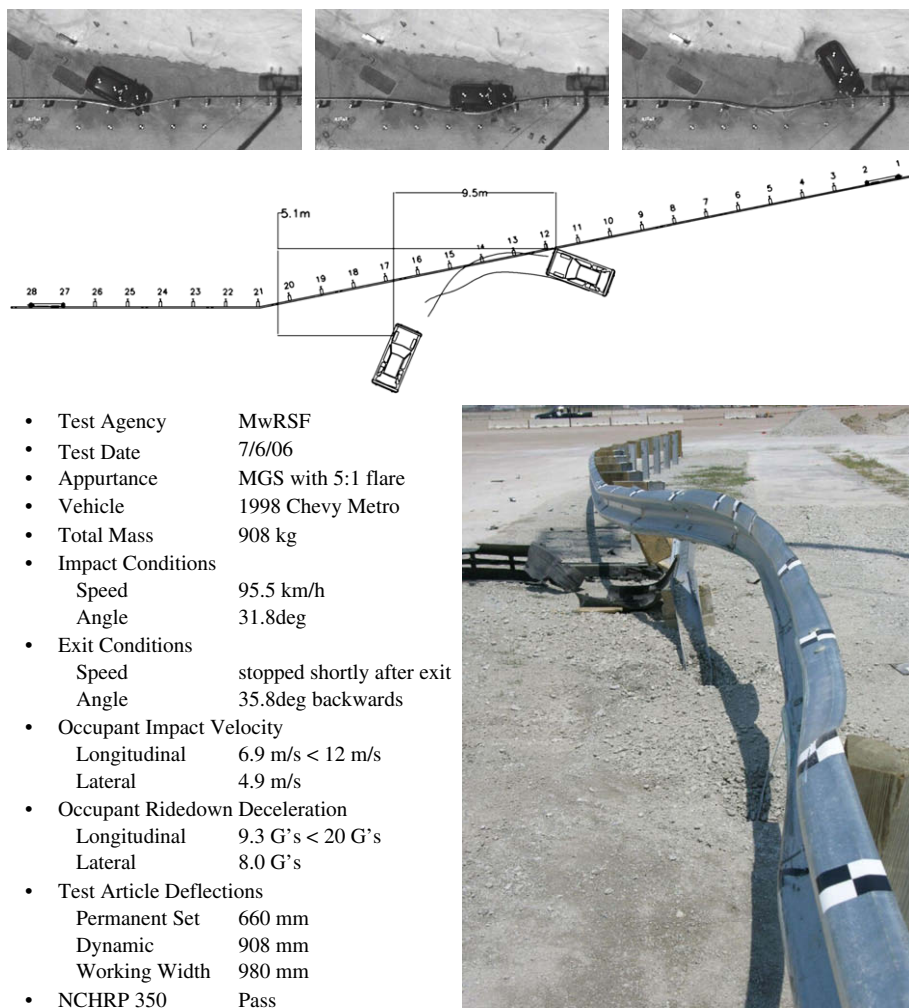


Fig. 8. Test FR-5 summary.

Hence, impacts just upstream of the hinge point are not believed to be a concern.

Another concern that has been expressed regarding implementation of the research described herein is the presence of roadside slopes. Clearly W-beam guardrail cannot be used on roadside slopes steeper than 8:1. Steeper flare rates cannot be utilized when the flare would extend onto such a slope. Nevertheless, the steeper flare rates recommended herein will provide improved safety performance at a reduced cost whenever roadside slopes are 10:1 or flatter. Note that recent crash testing has indicated that the MGS can be safely installed on 8:1 slopes. However, sufficient study has not been undertaken to determine whether it is appropriate to install a flared MGS guardrail on an 8:1 slope.

As described above, the effective impact angle increases as the guardrail flare rate increases. A vehicle encroaching at an angle of 25° from the roadway would strike 15:1 and 5:1 flared guardrail terminals at effective impact angles of 28° and 36°, respectively. It is generally believed that no existing guardrail terminals will be capable of sustaining an impact near the beginning of LON at either of these effective impact angles. In fact NCHRP Report 350 only requires terminals to be tested at an impact angle of 20°, instead of the 25° impact angle required for the guardrail itself. This reduced requirement for redirective capacity at the beginning of the LON for guardrail terminals is, in part, based upon recognition of the small window of vulnerability associated with this type of impact. Hence, increasing the recommended flare

rate does not introduce a new inconsistency in guardrail terminal testing and installed configuration.

The concept behind using high flare rates has always been that the reduction in impacts obtained by reducing the barrier length will outweigh the increase in accident costs associated with a modest increase in barrier penetrations. Research into the cost-effectiveness of flaring temporary concrete barriers clearly indicated that reducing the number of barrier crashes more than outweighed a relatively significant increase in both impact severities and barrier penetrations [2]. Research findings presented above clearly indicate that both impact severities and barrier penetration rates will not increase greatly, even with guardrail flare rates as high as 5:1. Note that there may be a significant increase in penetration rates for impacts very near the beginning of the LON for the terminal. However, this region of vulnerability is small in comparison to the overall guardrail installation and cannot be considered to represent a major increase in overall barrier penetration rate.

Additional research for flare rates could include a more thorough investigation into the topics listed in this section along with research into flare rates for other types of barrier systems.

Of near term interest would be a similar flare rate study investigating the updated NCHRP 350 procedures, known as MASH08. In MASH08 Tests 3–11 the pickup was changed from a 2000 kg two-door pickup to a 2270 kg four-door pickup, and in Test 3–10 the small car was changed from a 920 kg vehicle to a 1100 kg vehicle. Additionally, the impact angle in Test 3–10 was changed from 20° to

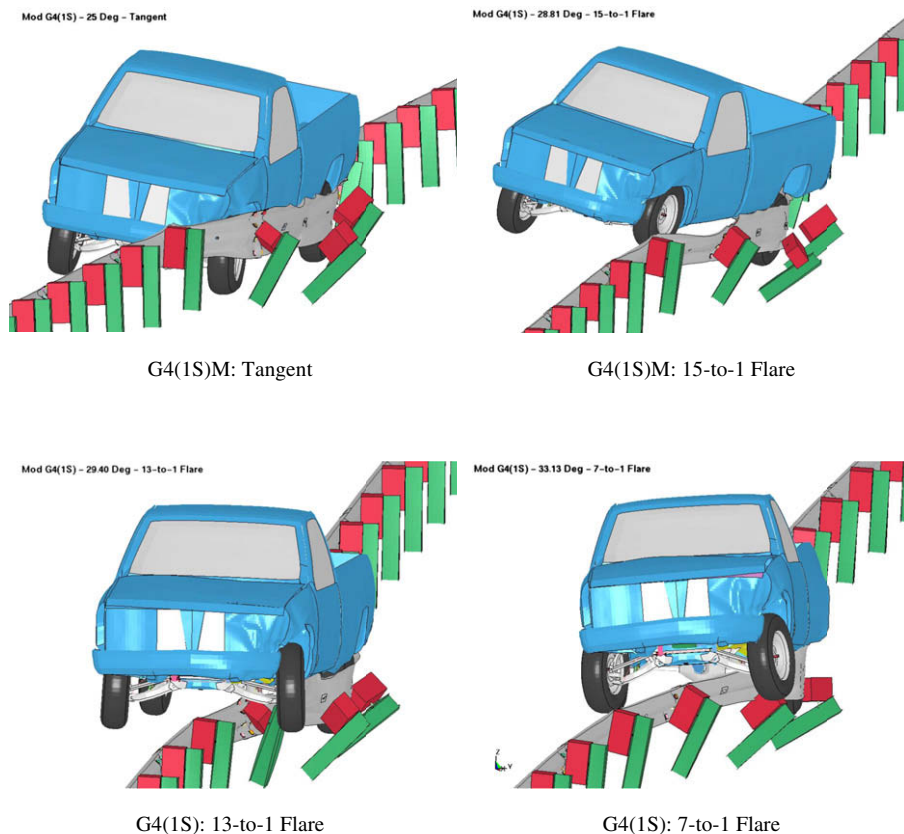


Fig. 9. G4(1S)M simulated flare rates.

25°. It is believed that these are significant enough changes to prohibit making any preliminary conclusions in regards to flare rates on the MGS MASH08 approved system.

8. Summary and conclusions

Whenever roadside or median slopes are relatively flat (10:1 or flatter), increasing the flare rate on guardrail installations becomes practical and has some major advantages including significantly reducing guardrail lengths and associated costs. Hence, a revised flare rate design has the potential to decrease construction, maintenance, and overall accident costs, provided guardrail accident severities are not increased significantly.

Although computer simulations indicate that conventional G4(1S)M guardrail cannot perform effectively when installed at flare rates higher than 15:1, the MGS has been shown to provide adequate protection for motorists when installed at flare rates of up to 5:1. Crash testing results, as well as LS-DYNA simulations, for both the 2000p pickup truck and 820c small car on the MGS installed with multiple flare rates demonstrated excellent performance. All tests conducted up to, and including on, a flare rate of 5:1 passed all NCHRP 350 safety performance evaluation requirements, including occupant risk measures that are not specifically required for Test 3–11 and including not redirecting any vehicles back into the roadway into adjacent traffic. Additionally, all tests had higher impact angles and speeds than those specified in NCHRP 350, resulting in even higher effective flare rates than intended. These tests indicate that the MGS is a very robust system when installed in a flared configuration.

Based upon the series of full-scale crash tests described herein, it is recommended that, whenever roadside topography permits, much steeper flare rates, up to 5:1, should be considered for MGS

installations. These steeper flare rates will reduce overall accident frequencies, overall accident costs and total construction costs, without sacrificing guardrail redirective capacity. Hence, implementing findings from this study should not only improve roadside safety, but also reduce guardrail construction and repair costs.

Acknowledgments

The authors wish to acknowledge the Midwest State's Regional Pooled Fund Program and the National Cooperative Research Project for sponsoring this project. In addition, the authors wish to acknowledge the MwRSF staff for conducting the crash tests and providing other valuable services for this project. An acknowledgement also goes to LSTC, the developers and providers of LS-DYNA. The simulation work performed during this project was completed utilizing the Research Computing Facility of the University of Nebraska–Lincoln.

References

- [1] Ross HE, Sicking DL, Zimmer RA, Michie JD. Recommended procedures for the safety performance evaluation of highway features. National Cooperative Research Program (NCHRP) report no. 350. Washington, DC: Transportation Research Board; 1993.
- [2] Ross Jr HE, Krammes RA, Sicking DL, Tyer KD, Perera HS. Traffic barriers and control treatments for restricted work zones. National Cooperative Highway Research Program report 358. Washington, DC: Transportation Research Board; 1994.
- [3] American Association of State Highway and Transportation Officials (AASHTO). Roadside design guide. Chapter 5 roadside barrier, section 5.6.3 flare rate. Washington, DC: AASHTO; 2002. p. 5–21.
- [4] Reid JD, Sicking DL, Faller RK, Pfeifer BG. Development of a new guardrail system. In: Transportation research record 1599. Washington, DC: TRB, National Research Council; September 1997. p. 72–80.

- [5] Sicking DL, Reid JD, Rohde JR. Development of the midwest guardrail system. In: Transportation research record 1797. Washington, DC: TRB, National Research Council; November 2002. p. 44–52.
- [6] Kuipers BD, Faller RK, Reid JD. Critical flare rates for W-beam guardrail – determining maximum capacity using computer simulation. MwRSF research report TRP-03-157-04. Lincoln, NE: University of Nebraska; January 24, 2005.
- [7] Faller RK, Polivka KA, Kuipers BD, Bielenberg RW, Reid JD, Rohde JR, Sicking DL. Midwest guardrail system for standard and special applications. In: Transportation research record 1890. Washington, DC: TRB, National Research Council; 2004. p. 19–33.
- [8] Powell GH. BARRIER VII: a computer program for evaluation of automobile barrier systems. Prepared for: federal highway administration. Report No. FHWA RD-73-51; April 1973.
- [9] Hallquist JO. LS-DYNA keyword user's manual. Version 970. Livermore, CA: Livermore Software Technology Corporation; April, 2003.
- [10] Bullard Jr DL, Menges WL, Alberson DC. NCHRP report 350 compliance test 3–11 of the modified G4(1S) guardrail with timber blockouts. Report no. FHWA-RD-96-175. College Station, TX: Texas Transportation Institute, Texas A&M University; September 1996.
- [11] Polivka KA, Sicking DL, Rohde JR, Faller RK, Holloway JC. Crash testing of Michigan's type B (W-Beam) guardrail system. MwRSF research report TRP-03-90-99. Lincoln, NE: University of Nebraska; November 10, 1999.
- [12] Polivka KA, Sicking DL, Rohde JR, Faller RK, Holloway JC. Crash testing of Michigan's type B (W-beam) guardrail system – phase II. MwRSF research report TRP-03-104-00. Lincoln, NE: University of Nebraska; December 13, 2000.